Riemann problems and dispersive shocks in self-focusing media

Gino Biondini

Department of Physics, State University of New York at Buffalo, Buffalo, New York 14260, USA
and Department of Mathematics, State University of New York at Buffalo, Buffalo, New York 14260, USA

The dynamical behavior resulting from an initial discontinuity in focusing media is investigated using a combination of numerical simulations and Whitham modulation theory for the focusing nonlinear Schrödinger equation. Initial conditions with a jump in either or both the amplitude and the local wave number are considered. It is shown analytically and numerically that the space-time plane divides into expanding domains in which the solution is described by a slow modulation of genus-0, genus-1 or genus-2 solutions, their precise arrangement depending on the specifics of the initial datum.

I. INTRODUCTION

The study of Riemann problems—i.e., the evolution of a jump discontinuity between two uniform values of the initial datum—is a well-established part of fluid dynamics, since understanding the response of a system to such kinds of inputs is a key step in characterizing its behavior [1,2]. When nonlinearity and dissipation are the dominant physical effects, these problems can give rise to classical shocks [2,3]. When dissipation is negligible compared to dispersion, however, Riemann problems can give rise to dispersive shock waves (DSWs). The study of dispersive hydrodynamics has attracted considerable attention in recent years [4]. Here we are interested in Riemann problems and DSW formation in self-focusing media.

A universal model for nonlinear focusing media is the one-dimensional cubic nonlinear Schrödinger (NLS) equation, which describes modulations of weakly nonlinear dispersive wave trains in many different physical contexts, such as deep water waves, optical fibers, plasmas, and attracting Bose-Einstein condensates [5–8]. The NLS equation is a completely integrable system, and it can be studied via the inverse scattering transform (IST) [8–11]. Several related studies using the IST have appeared in recent years [12–19]. On the other hand, a simpler approach is Whitham modulation theory [4,20]. The latter does not require integrability, and therefore it is not restricted to completely integrable systems such as the NLS equation, and it can be extended to more general self-focusing dynamical systems such as those studied in [21].

Whitham theory has been used extensively to study Riemann problems in defocusing media [22–26]. A few works have also used Whitham equations in focusing media [27–29], and a few attempts have been made to combine it with the IST [19,28,30], but it is fair to say that the corresponding theory is much less developed than for defocusing media. The main reason for this situation is that, while the Whitham equations for the defocusing NLS equation are hyperbolic, those for the focusing NLS equation are elliptic, and are therefore unsuitable to study initial value problems (IVPs) in general. Nonetheless, here we demonstrate how, despite this

difficulty, a relatively broad class of Riemann problems can still be effectively studied using Whitham modulation theory.

II. NLS EQUATION AND ITS WHITHAM EQUATIONS

We begin by reviewing some background material, to set up the relevant framework. We write the one-dimensional focusing NLS equation with small dispersion as

$$i\epsilon q_t + \epsilon^2 q_{xx} + 2|q|^2 q = 0, \tag{1}$$

where subscripts x and t denote partial differentiation and $0 < \epsilon \ll 1$ is a small parameter that quantifies the relative strength of dispersion compared to nonlinearity. Recall that Eq. (1) possesses several invariances: phase rotations, spatial reflections, scaling, and Galilean transformation. Specifically, if $q(x,t)$ is any solution of Eq. (1), so are $e^{i\alpha}q(x,t), q(-x,t)$, $aq(ax, a^2 t)$ and $e^{i(Vx-V^2t)}q(x - Vt, t)$, where all transformation parameters are real-valued. All of these invariances will be useful below.

As is well known, the so-called Madelung transformation, namely

$$q(x,t) = \sqrt{\rho(x,t)}\, e^{iS(x,t)/\epsilon}, \tag{2}$$

where the real-valued quantities $\rho(x,t)$ and $S(x,t)$ represent respectively the local intensity and local phase, transforms Eq. (1) into the hydrodynamic-type system

$$\frac{\partial \rho}{\partial t} = \frac{\partial(\rho v)}{\partial x}, \tag{3a}$$

$$\frac{\partial(\rho v)}{\partial t} = \frac{\partial}{\partial x}\left(\rho v^2 - \frac{1}{2}\rho^2 - \frac{1}{4}\epsilon^2 \rho \frac{\partial^2}{\partial x^2}\ln \rho\right), \tag{3b}$$

where $S_x(x,t) = v(x,t)$ is the local wave number. The truncation $\epsilon = 0$ of Eqs. (3) is the genus-0 NLS-Whitham system. Recall that Eq. (1) admits the background solution $q(x,t) = q_o e^{2iq_o^2 t}$, together with its generalizations via the above-mentioned invariances. The system (3) describes slow modulations of such a solution.

In addition to constant and soliton solutions, the focusing NLS equation (1) also admits solutions describing periodic,

traveling wave solutions in the form [29]

$$|q(x,t)|^2 = (\alpha_{\mathrm{im}} + \gamma_{\mathrm{im}})^2 - 4\alpha_{\mathrm{im}}\gamma_{\mathrm{im}}\,\mathrm{sn}^2[C(x-Vt);m], \quad (4)$$

where $\mathrm{sn}(\cdot)$ is a Jacobi elliptic function [31], and the elliptic parameter m and the constants C and V are

$$m = 4\alpha_{\mathrm{im}}\gamma_{\mathrm{im}}/|\alpha-\gamma|^2, \quad C = |\alpha-\gamma|, \quad V = 2(\alpha_{\mathrm{re}} + \gamma_{\mathrm{re}}), \tag{5}$$

with $\alpha = \alpha_{\mathrm{re}} + i\alpha_{\mathrm{im}}$, $\gamma = \gamma_{\mathrm{re}} + i\gamma_{\mathrm{im}}$. Note that α, α^*, γ, and γ^* are the branch points of the spectrum of the scattering problem associated to Eq. (1) [32].

A system of modulation equations for the above periodic solutions of the focusing NLS Eq. (1) when $0 < \epsilon \ll 1$ can be obtained via Whitham averaging theory [20]. The result is the genus-1 NLS-Whitham system [33,34]. Explicitly, in Riemann invariant coordinates,

$$\frac{\partial r_j}{\partial t} + V_j\,\frac{\partial r_j}{\partial x} = 0, \quad j = 1,\dots,4, \tag{6}$$

where $r_1,\dots,r_4$ are the Riemann invariants, and the characteristic velocities are

$$V_j = V + W_j, \quad j = 1,\dots,4, \tag{7}$$

where $V = r_1 + r_2 + r_3 + r_4$, with

$$W_1 = 2\Delta_{12}/[1 - (\Delta_{24}/\Delta_{14})\,R(m)], \tag{8a}$$

$$W_3 = 2\Delta_{34}/[1 - (\Delta_{24}/\Delta_{23})\,R(m)], \tag{8b}$$

$$\Delta_{jk} = r_j - r_k, \quad j,k = 1,\dots,4, \tag{8c}$$

$W_2 = W_1^*$, $W_4 = W_3^*$, and $R(m) = E(m)/K(m)$, where $K(m)$ and $E(m)$ are the complete elliptic integrals of the first and second kind, respectively [31]. Importantly, the Riemann invariants are exactly the branch points of the elliptic solution (4). That is, $r_1 = \alpha$, $r_2 = \alpha^*$, $r_3 = \gamma$, and $r_4 = \gamma^*$.

The NLS Eq. (1) also admits multiphase solutions [32]. In general, genus-g solutions are expressed as ratios of Jacobi theta functions [35], and their modulations are described by corresponding genus-g Whitham modulation systems [33,34]. We refer the reader to [19] for a review. We will not use such higher-genus solutions and the corresponding modulation systems here.

III. RIEMANN PROBLEMS FOR THE FOCUSING NLS EQUATION

The Whitham equations for Eq. (1) are elliptic, and the Riemann invariants and the characteristic velocities are in general complex valued. Hence, these systems cannot be used to study IVPs in general, contrary to the defocusing case. Nonetheless, we next show that, notwithstanding this difficulty, the system (6) still yields useful information about the behavior of solutions of Eq. (1).

We consider the focusing NLS equation with the following class of initial conditions (ICs):

$$q(x,0) = \begin{cases} A_-\,e^{i\mu x/\epsilon - i\phi/\epsilon}, & x < 0, \\ A_+\,e^{-i\mu x/\epsilon + i\phi/\epsilon}, & x > 0, \end{cases} \tag{9}$$

with $A_\pm \geqslant 0$ and μ and ϕ real, and we classify the resulting dynamics depending on the values of $A_\pm$ and μ. (It turns out that the value of ϕ has no effect on our results.) The results can be considered the analog for the focusing case of those obtained in [24] for the defocusing case.

Nonzero values of μ correspond to the presence of carriers with opposite wave numbers for $x < 0$ and $x > 0$, which, due to the Galilean invariance of the NLS equation, induce counterpropagating flows. For $\mu > 0$, the two halves of the IC (9) propagate inward (i.e., towards each other), whereas for $\mu < 0$ they flow outward (i.e., away from each other). Note that one can always take the discontinuity at $x = 0$ and set the phases of the IC for $x < 0$ and $x > 0$ to be equal and opposite without loss of generality, thanks to the translation and phase invariance of the NLS equation. Similarly, one can always take the carrier wave numbers for $x < 0$ and $x > 0$ to be equal and opposite thanks to the Galilean invariance of the NLS equation.

IV. ONE-SIDED STEP

The simplest scenario of ICs given by Eq. (9) is that of a one-sided step, in which $A_- = 0$. Then we can always set $A_+ > 0$ and $\mu = \phi = 0$ without loss of generality thanks to the phase and Galilean invariances of Eq. (1). The long-time asymptotics of solutions generated by these ICs was studied in [14] by IST. On the other hand, the dynamics can be effectively described via the genus-1 Whitham system (6) [19].

Even though the Riemann invariants and the characteristic velocities are in general complex, the genus-1 system (6) does possess some real-valued solutions. In particular, it admits the self-similar solution [27]

$$4\alpha_{\mathrm{re}} + 2(A_+^2 - \alpha_{\mathrm{im}}^2)/\alpha_{\mathrm{re}} = \xi, \qquad \gamma = iA_+, \tag{10a}$$

$$[\alpha_{\mathrm{re}}^2 + (A_+ - \alpha_{\mathrm{im}})^2]\,K(m) = (\alpha_{\mathrm{re}}^2 - \alpha_{\mathrm{im}}^2 + A_+^2)\,E(m), \tag{10b}$$

with $\xi = x/t$. This solution describes a slow modulation of the elliptic solution (4) [now describing oscillations with characteristic spatial period $O(\epsilon)$, as can be easily seen by performing a simple rescaling of the spatial and temporal variables in Eq. (1) when $\epsilon \neq 1$]. As discussed in [19], Eqs. (10) correctly capture the behavior of the solution of the NLS Eq. (1) with IC (9) for $0 < x < 4\sqrt{2}A_+t$. For $x > 4\sqrt{2}A_+t$, the solution of the Whitham system is simply given by $\gamma = iA_+$ and $\alpha = 0$, which matches the limit of the self-similar solution (10), and which yields the constant solution $q(x,t) = A_+$ of the NLS equation (up to a uniform phase). Finally, for $x < 0$ the solution of the NLS equation is described by the degenerate, constant genus-0 solution $\gamma = \alpha = 0$ of the Whitham system (6), which yields the trivial solution $q(x,t) = 0$ of the NLS equation. Summarizing, the solution (10) describes an oscillatory wedge $V_-t < x < V_+t$, with $V_- = 0$ and $V_+ = 4\sqrt{2}A_+$, which connects the constant solution $q(x,t) = 0$ to its left to the constant solution $q(x,t) = A_+$ to its right.

The actual behavior of the solutions of the NLS equation with the above IC [36] is shown in Fig. 1 together with the
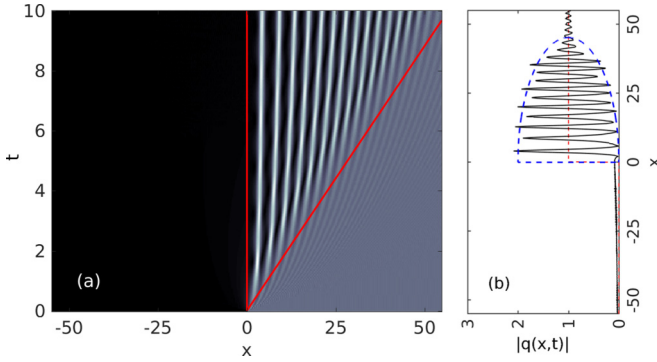
FIG. 1. (a) Density plot of the amplitude $|q(x, t)|$ of the solution of the focusing NLS Eq. (1) with $\epsilon = 1$ generated by a one-sided step IC (9) with $A_- = \mu = 0$ and $A_+ = 1$, together with the boundaries (red lines) between the genus-0 and genus-1 regions predicted by Whitham theory. (b) $|q(x, t)|$ (solid black line) as a function of x at $t = 8$, together with the IC (9) (dashed red line) and the envelope of the oscillations predicted by Whitham theory (dashed blue lines).

predictions from Whitham theory, demonstrating excellent agreement. (The grayscale used for all density plots in this work is shown in Fig. 2.) Importantly, note that the velocity of the matching point between the two solutions is zero, i.e., the discontinuity is pinned at $x = 0$, unlike what happens in the defocusing case [23].

V. SYMMETRIES

Importantly, the invariances of the NLS equation induce corresponding symmetries for the Whitham equations. (This is similar to what happens for other nonlinear evolution equations, even in two spatial dimensions; e.g., see [37].)

Specifically, the Whitham modulation equations (and therefore the Riemann invariants) are insensitive to (i.e., invariant under) uniform phase rotations of the solutions of the NLS equation [i.e., under transformations $q'(x, t) = q(x, t) e^{i\phi}$, with ϕ an arbitrary real constant]. Spatial translations of the solution of the NLS equation [i.e., transformations $q'(x, t) = q(x - X_o, t)$, with X_o an arbitrary real constant] simply result in corresponding translations of the Riemann invariants [that is, $\alpha'(x, t) = \alpha(x - X_o, t)$ and $\gamma'(x, t) = \gamma(x - X_o, t)$]. Spatial reflections [i.e., the transformation $q'(x, t) = q(-x, t)$] simply yield a reflection of the Riemann invariants [that is, $\alpha'(x, t) = \alpha(-x, t)$ and $\gamma'(x, t) = \gamma(-x, t)$]. The invariance under scaling transformations [i.e., transformations $q'(x, t) = aq(ax, a^2t)$, with a an arbitrary real constant] yields a corresponding scaling for the Riemann invariants [that is, $\alpha'(x, t) = a\alpha(ax, a^2t)$ and $\gamma'(x, t) = a\gamma(ax, a^2t)$]. Finally, Galilean boosts also translate to a corresponding transformation for the Riemann invariants. That is, letting $q'(x, t) = q(x - 2V_ot, t) e^{i(V_ox - 2V_o^2t)}$ (with V_o an arbitrary real constant) yields $\gamma'(x, t) = V_o + \gamma(x - 2V_o t, t)$ and $\alpha'(x, t) = V_o + \gamma(x - 2V_o t, t)$. (Interestingly, the induced
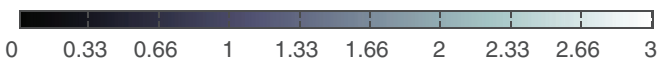

FIG. 2. The grayscale used for all the density plots in this work.
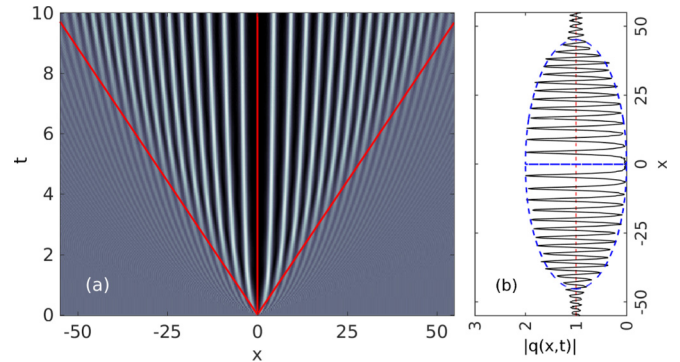
transformation for the Riemann invariants is essentially the same as in the corresponding symmetries of the Whitham equations for the KdV equation, even though the transformation of the solutions of the two PDEs is very different [4].)

The combination of the above invariances and the pinning of the discontinuity at $x = 0$ for the self-similar solution (10) arising from the one-sided step IC (9) is the key that enables us to use the above solution to analyze the more complicated scenarios, as we discuss next. In particular, note that multiplying Eq. (9) by e^{iV_ox} results in a slanted oscillatory wedge with boundaries at $x = V_\pm t$, where now $V_- = 2V_o$ and $V_+ = 2V_o + 4\sqrt{2}A_+$.

VI. SYMMETRIC TWO-SIDED STEP

Consider now a two-sided step given by the IC (9) with $A_- = A_+$ and $\mu = 0$, corresponding to an initial phase discontinuity at $x = 0$. Without loss of generality we can set $A_\pm = 1$ thanks to the scaling invariance of the NLS equation.

One can view the above IC as a superposition of two one-sided steps. Of course the solution of the NLS equation is not simply given by a superposition of the corresponding one-sided solutions in general. Nonetheless, the property holds for the Whitham system in this case, thanks to the invariances of the one-sided solution, the fact that the discontinuity of one-sided wedge is pinned at the origin, and that the solution to the left of the wedge is asymptotically zero. Thus, the solution of the genus-1 Whitham system generated by the above IC is simply the linear superposition of the evolution of the one-sided step discussed above and that of a reflected step.

The resulting behavior is shown in Fig. 3, again demonstrating excellent agreement. Note that the Whitham system is insensitive to the phase of $q(x, t)$ and hence to the value of ϕ. In particular, when $\phi = 0$ the IC has no discontinuity at $x = 0$; this is the case considered in [27]. But a similar behavior arises in the presence of a jump discontinuity in the phase of the IC.

It was suggested in [27] that the self-similar solution (10) describes the evolution of small perturbations of the constant background as a result of modulational instability. And indeed it was shown in [16,18] using IST that the long-time asymptotics of a very broad class of IC corresponding to localized perturbations of a constant background tends asymptotically
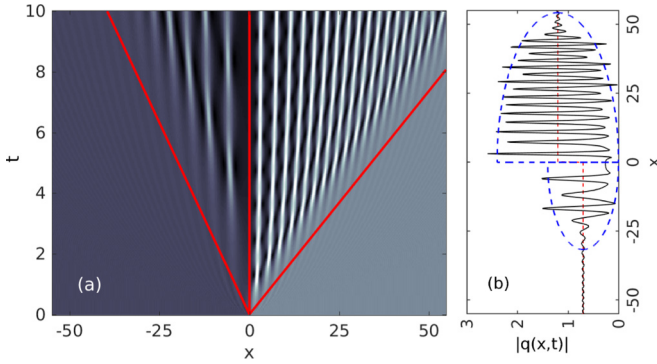

FIG. 3. Same as Fig. 1, but for a two-sided step IC given by (9) with $A_- = A_+ = 1$, $\phi = \pi/2$, and $\mu = 0$.

FIG. 4. Same as Fig. 1, but for an asymmetric two-sided step IC (9) with $A_- = 0.7$, $A_+ = 1.2$, and $\mu = \phi = 0$.

to this behavior as $t \to \infty$. The properties of the self-similar solution were further studied in [17]. Next we show how suitable combinations of the above one-sided solutions allow one to study even more general scenarios.

VII. ASYMMETRIC TWO-SIDED STEP

We now consider the case $A_\pm \neq 0$ and $A_- \neq A_+$, which we refer to as an asymmetric step. Without loss of generality we can take $A_- < A_+$, owing to the invariance of the NLS equation with respect to spatial reflections.

As before, one can view these IC as a superposition of two one-sided steps, but now with different amplitude. As a result, the solution of the corresponding IVP for the Whitham equation is again given by the superposition of two one-sided self-similar solutions. Note however that now the two halves have a different amplitude and different propagation speed. An example of the resulting behavior is shown in Fig. 4 for $A_- = 0.7$ and $A_+ = 1.2$, demonstrating once more excellent agreement between the self-similar solutions of the Whitham equations and the numerical solution of the NLS equation.

VIII. OUTWARD COUNTERPROPAGATING FLOWS

We now consider a different generalization of a symmetric two-sided step by allowing for the presence of counterpropagating flows, which are obtained when $\mu \neq 0$. We first discuss the case of symmetric outward flows; that is, we consider the IC (9) with $A_- = A_+ = A$ and $\mu < 0$. Again, without loss of generality we can take $A = 1$ thanks to the scaling invariance of the NLS equation.

As before, it is useful to look at the IC as a superposition of two one-sided steps. Because of the presence of a nonzero wave number, however, in this case the discontinuity for each solution half does not remain pinned at $x = 0$, but instead travels to the left or to the right with speed $2|\mu|$. More precisely, the discontinuity in the left half is now located at $x = -2|\mu|t$ and the one in the right half at $x = 2|\mu|t$. As a result, a wedge-shaped vacuum zone develops in the central portion of the xt plane, i.e., for $|x| < 2|\mu|t$. An example of the behavior resulting from the above IC is shown in Fig. 5 for $\mu = -0.5$, demonstrating again excellent agreement with the corresponding solution of the Whitham equations.
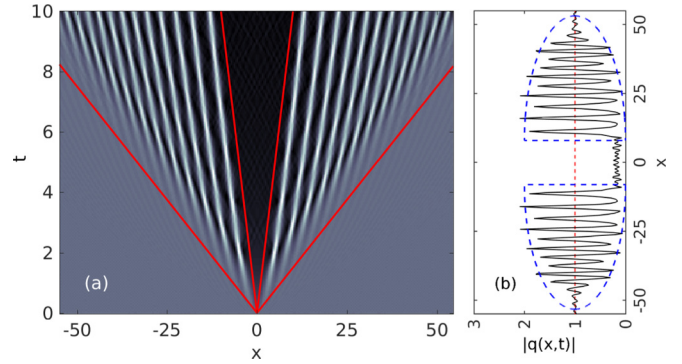

FIG. 5. Same as Fig. 1, but for outward counterpropagating flows given by the IC (9) with $A_\pm = 1$ and $\mu = -0.5$.

A similar outcome is obtained when the ICs combine outward counterpropagating flows with an asymmetric step (i.e., an amplitude discontinuity), i.e., from Eq. (9) with $0 < |A_-| < |A_+|$ and $\mu < 0$. Indeed, Fig. 6 shows such a case, obtained with $A_- = 0.7$, $A_+ = 1.2$, and $\mu = -0.5$, demonstrating once more excellent agreement between the Whitham equations and numerical solutions of the NLS equation.

IX. INWARD COUNTERPROPAGATING FLOWS

A different outcome is obtained when inward counterpropagating flows are present, namely when $\mu > 0$. In this case, the nonzero carrier causes the two halves of the solution to travel toward each other. In particular, the two individual solutions overlap in the region $|x| < 2\mu t$.

An example of the resulting behavior for $A_\pm = 1$ and $\mu = 0.5$ is shown in Fig. 7. The dot-dashed lines in Fig. 7(b) indicate the boundary of the overlap region. Inside this region, the interaction between the two genus-1 regions presumably results in the formation of a genus-2 region (similarly to what happens in the defocusing case [25,26]), so the asymptotic expression for the solution in this region will be described by a slow modulation of the genus-2 solutions of the NLS equation, and one cannot obtain useful information in this region using the genus-1 Whitham equations.

Regions with more complicated oscillation patterns are indeed clearly visible in Fig. 7. [The appearance of genus-2
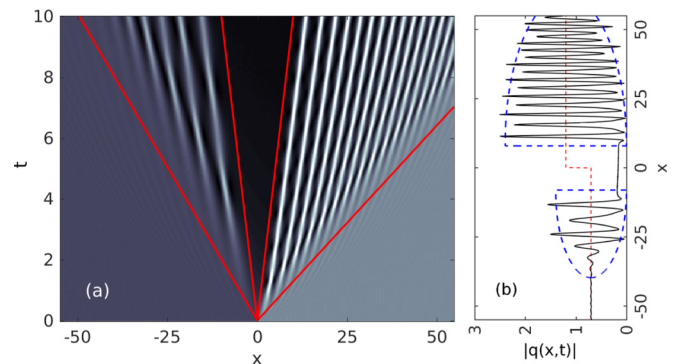

FIG. 6. Same as Fig. 1, but for an IC consisting of outward counterpropagating flows with unequal amplitude, given by Eq. (9) with $A_- = 0.7$, $A_+ = 1.2$, and $\mu = -0.5$.
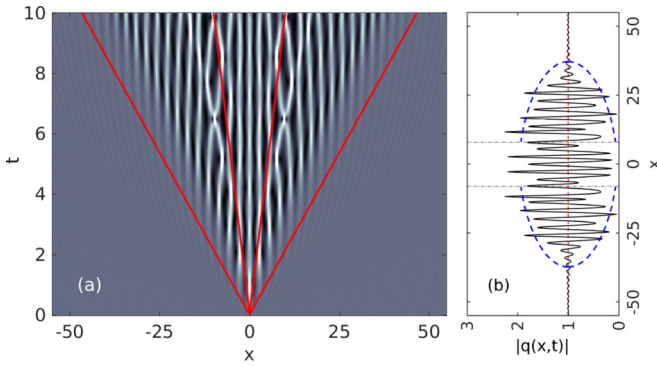
FIG. 7. Same as Fig. 1, but for inward counterpropagating flows given by the IC (9) with $A_\pm = 1$ and $\mu = 0.5$.

regions for this case had been predicted in [13] based on the calculation of the long-time asymptotics of solutions. Note, however, that [13] predicted a central genus-1 region surrounded by two genus-2 regions, each of which is directly adjacent to the outermost genus-0 regions, in contrast with the predictions from Whitham theory and the numerical results. Moreover, the boundary between the two genus-2 regions and the genus-0 regions was predicted to be at $x = \pm 2(\mu + A^2/\mu)t$, which is inconsistent with the limit $\mu \to 0$, since in that case the solution reduces to the symmetric two-sided step discussed earlier.] We also note that an even more complex scenario is obtained when $\mu > 2\sqrt{2}A$, since in that case the genus-1 Whitham equations predict that the DSW region generated by the left half of the IC would be completely to the right of the one generated by the right half, and vice versa. It is not possible to make any predictions for this case using only the genus-1 Whitham equations.

The last scenario we consider is that of an asymmetric step with inward counterpropagating flows, which is obtained from Eq. (9) by taking $0 < A_- < A_+$ and $\mu > 0$. This case yields a similar outcome to that of a symmetric step, the only differences being once again the amplitude inside the oscillation region and its expansion speed. The corresponding solution is shown in Fig. 8. Interestingly, however, the difference between the genus-1 and genus-2 regions is more clearly identifiable in this case compared to that of a symmetric step.
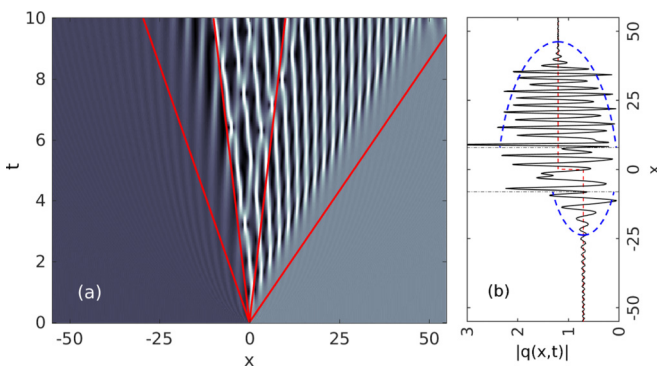

FIG. 8. Same as Fig. 1, but for an IC consisting of inward counterpropagating flows with unequal amplitude, given by Eq. (9) with $A_- = 0.7$, $A_+ = 1.2$, and $\mu = 0.5$.

We do not have a simple explanation for why this should be the case. As before, more complicated outcomes can be obtained when larger values of μ are considered. In this case, however, we expect two different thresholds, one at $\mu = 2\sqrt{2}A_-$ and one at $\mu = 2\sqrt{2}A_+$.

X. DISCUSSION

In summary, we proposed a classification of the dynamical scenarios generated by a single jump in the IC for the focusing NLS equation in the semiclassical limit. The first few cases had been studied before, either by Whitham theory or by the IST. In particular, the self-similar solution of the genus-1 Whitham equations derived in [27] was used in [28] to present a qualitative description of the solutions produced by the inward and outward counterpropagating flow ICs discussed above. Note, however, that no actual solutions of the NLS equation (either exact or numerical) were reported in [28]. Thus, a quantitative comparison between the predictions of Whitham theory and the actual solutions of the NLS equation was still missing. This is surprising, since, in the defocusing case, similar problems, as well as much more complicated ones, have been well characterized [23–26].

While in this work the problem was formulated in the framework of semiclassical limits, there is a well-known correspondence between small dispersion limits (described by Whitham theory) and long-time asymptotics, which applies whenever the ICs considered are scale invariant, and the IC (9) studied in this work does possess this property.

There are marked differences between the behavior resulting from an initial discontinuity in the focusing versus the defocusing case. In the defocusing case, a single discontinuity generates at most genus-1 regions [22], and one can only obtain genus-2 regions when two or more such discontinuities are considered [25,26]. Here, instead, we have seen that expanding genus-2 regions are generated when the IC contains inward counterpropagating flows (as in Figs. 7 and 8).

Unlike what happens in other situations in both the focusing and defocusing cases [12,25,26,38,39], here the boundaries of the genus-2 regions are not curved, but straight lines instead. This is because of the scaling invariance of the IC considered here, which makes the semiclassical limit equivalent to the long-time asymptotics.

Whitham theory appears to slightly overestimate the spatial extent of the oscillation regions in some cases. Recall that small deviations between the predictions of Whitham theory and the actual PDE behavior are known to arise in the linear limit [4] of the former. Moreover, all numerical computations in this work were done with $\epsilon = 1$, while Whitham theory is designed to capture the behavior of solutions as $\epsilon \to 0$, so one would not necessarily expect the latter to be effective for such large values of ϵ. Perhaps better agreement could be attained for smaller values of ϵ. But, given the ellipticity of the Whitham equations in the focusing case, we find it quite remarkable that Whitham theory is even effective at all in the various situations considered here.

In fact, while in the defocusing case one can prove that the solutions of the Whitham equations provide an asymptotic approximation for the time evolution of the corresponding

IC for the NLS equation, the same is not possible in the focusing case since in this case the Whitham equations are elliptic. The situation is the same as in the cases studied in [19,27]. Therefore, a rigorous description of the problems studied here can be obtained by computing the long-time asymptotics via the IST, which will also be necessary to quantitatively describe the solution in the various genus-2 regions as well as in the cases when the genus-1 Whitham equations yield no predictions whatsoever (e.g., in the case of inward counterpropagating flows when $\mu > 2\sqrt{2}A$).

On the other hand, we reiterate that since Whitham theory does not require integrability, the results of this work are expected to also be applicable to many other NLS-type evolution equations that are not integrable, such as the ones considered in [21], which means that they should be experimentally observable in one of the various physical settings in which these models arise. Indeed, experimental observation of some of the scenarios discussed in this work have already recently been reported in [40]. It is therefore hoped that the remaining ones will also be realized experimentally in the future.

[1] R. Courant and D. Hilbert, *Methods of Mathematical Physics* (Interscience, New York, 1962).

[2] P. D. Lax, *Hyperbolic Systems of Conservation Laws and the Mathematical Theory of Shock Waves* (SIAM, Philadelphia, 1973).

[3] R. Courant and K. O. Friedrichs, *Supersonic Flow and Shock Waves* (Springer-Verlag, New York, 1976).

[4] G. A. El and M. A. Hoefer, Dispersive shock waves and modulation theory, Phys. D (Amsterdam, Neth.) **333**, 11 (2016).

[5] G. P. Agrawal, *Nonlinear Fiber Optics* (Academic, New York, 2001).

[6] E. Infeld and G. Rowlands, *Nonlinear Waves, Solitons and Chaos* (Cambridge University Press, Cambridge, UK, 2000).

[7] L. P. Pitaevskii and S. Stringari, *Bose-Einstein Condensation* (Clarendon, Oxford, 2003).

[8] M. J. Ablowitz and H. Segur, *Solitons and the Inverse Scattering Transform* (SIAM, Philadelphia, 1981).

[9] S. P. Novikov, S. V. Manakov, L. P. Pitaevskii, and V. E. Zakharov, *Theory of Solitons: The Inverse Scattering Transform* (Plenum, New York, 1984).

[10] L. D. Faddeev and L. A. Takhtajan, *Hamiltonian Methods in the Theory of Solitons* (Springer, Berlin, 1987).

[11] M. J. Ablowitz, B. Prinari, and A. D. Trubatch, *Discrete and Continuous Nonlinear Schrödinger Systems* (Cambridge University Press, Cambridge, UK, 2004).

[12] S. Kamvissis, K. D. T-R. McLaughlin, and P. D. Miller, *Semiclassical Soliton Ensembles for the Focusing Nonlinear Schrödinger Equation* (Princeton University Press, Princeton, 2003).

[13] R. Buckingham and S. Venakides, Long-time asymptotics of the nonlinear Schrödinger equation shock problem, Commun. Pure Appl. Math. **60**, 1349 (2007).

[14] A. Boutet de Monvel, V. P. Kotlyarov and D. Shepelsky, Focusing NLS equation: long-time dynamics of step-like initial data, Int. Math. Res. Not. **2011**, 1613 (2011).

[15] R. Jenkins and K. D. T.-R. McLaughlin, Semiclassical limit of focusing NLS for a family of square barrier initial data, Commun. Pure Appl. Math. **67**, 246 (2013).

[16] G. Biondini and D. Mantzavinos, Universal Nature of the Nonlinear Stage of Modulational Instability, Phys. Rev. Lett. **116**, 043902 (2016).

[17] G. Biondini, S. Li, and D. Mantzavinos, Oscillation structure of localized perturbations in modulationally unstable media, Phys. Rev. E **94**, 060201(R) (2016).

[18] G. Biondini and D. Mantzavinos, Long-time asymptotics for the focusing nonlinear Schrödinger equation with nonzero boundary conditions at infinity and asymptotic stage of modulational instability, Commun. Pure Appl. Math. **70**, 2300 (2017).

[19] G. A. El, E. G. Khamis, and A. Tovbis, Dam break problem for the focusing nonlinear Schrödinger equation and the generation of rogue waves, Nonlinearity **29**, 2798 (2016).

[20] G. B. Whitham, *Linear and Nonlinear Waves* (Wiley, New York, 1974).

[21] G. Biondini, S. Li, D. Mantzavinos, and S. Trillo, Universal behavior of modulationally unstable media, SIAM Rev. **60**, 888 (2018).

[22] G. A. El, V. V. Geogjaev, A. V. Gurevich, and A. L. Krylov, Decay of an initial discontinuity in the defocusing NLS hydrodynamics, Phys. D (Amsterdam, Neth.) **87**, 186 (1995).

[23] Y. Kodama and S. Wabnitz, Analytical theory of guiding-center NRZ and RZ signal transmission in normally dispersive nonlinear optical fibers, Opt. Lett. **20**, 2291 (1995).

[24] Y. Kodama, The Whitham equations for optical communications: mathematical theory of NRZ, SIAM J. Appl. Math. **59**, 2162 (1999).

[25] G. Biondini and Y. Kodama, On the Whitham equations for the defocusing nonlinear Schrödinger equation with step initial data, J. Nonlin. Sci. **16**, 435 (2006).

[26] M. A. Hoefer and M. J. Ablowitz, Interactions of dispersive shock waves, Phys. D (Amsterdam, Neth.) **236**, 44 (2007).

[27] G. A. El, A. V. Gurevich, V. V. Khodorovskii, and A. L. Krylov, Modulational instability and formation of a nonlinear oscillatory structure in a focusing medium, Phys. Lett. A **177**, 357 (1993).

[28] R. F. Bikbaev, Complex Whitham deformations in problems with integrable instability, Theor. Mat. Phys. **104**, 1078 (1995).

[29] A. M. Kamchatnov, *Nonlinear Periodic Waves and their Modulations* (World Scientific, Singapore, 2000).

[30] A. Tovbis and G. A. El, Semiclassical limit of the focusing NLS: Whitham equations and the Riemann-Hilbert problem approach, Phys. D (Amsterdam, Neth.) **333**, 171 (2016).

[31] F. W. Olver, D. W. Lozier, R. F. Boisvert, and C. W. Clark, *NIST Handbook of Mathematical Functions* (Cambridge University Press, Cambridge, UK, 2010).

[32] A. R. Its and V. P. Kotlyarov, Explicit formulas for solutions of a nonlinear Schrödinger equation, Dokl. Akad. Nauk Ukrain. SSR Ser. A **11**, 965 (1976).

[33] M. G. Forest and J.-E. Lee, Geometry and modulation theory for periodic nonlinear Schrödinger equation, in *Oscillation Theory, Computation and Methods of Compensated Compactness*, IMA Vol. Math.Appl. 2, edited by C. Dafermos, J. L. Ericksen, D. Kinderlehrer, and M. Slemrod (Springer, New York, 1986), pp. 35–69.

[34] M. V. Pavlov, Nonlinear Schrödinger equation and the Bogolyubov-Whitham method of averaging, Theor. Math. Phys. **71**, 584 (1987).

[35] X. Zhou, Riemann-Hilbert problems and integrable systems, MSRI Lectures, 1999.

[36] All numerical simulations of the NLS equation were performed using an eighth-order Fourier split-step code with 4096 spatial grid points, spatial domain $[-200, 200]$, and integration time step 10^{-4}.

[37] M. J. Ablowitz, G. Biondini and Q. Wang, Whitham modulation theory for the Kadomtsev-Petviashvili equation, Proc. R. Soc. London, Ser. A **473**, 20160695 (2017).

[38] P. D. Miller and S. Kamvissis, On the semiclassical limit of the focusing nonlinear Schrödinger equation, Phys. Lett. A **247**, 75 (1998).

[39] J. C. Bronski and J. N. Kutz, Numerical simulation of the semiclassical limit of the focusing nonlinear Schrodinger equation, Phys. Lett. A **254**, 335 (1999).

[40] A. E. Kraych, P. Suret, G. A. El and S. Randoux, Universal nonlinear stage of the locally induced modulational instability in fiber optics, arXiv:1805.05074.